CrossMark

ORIGINAL PAPER

Colorimetric determination of mercury(II) based on the inhibition of the aggregation of gold nanorods coated with 6-mercaptopurine

Ning Bi[1] · Meihua Hu[2] · Jun Xu[1] · Lei Jia[1]

Abstract The authors describe an optical assay for determination of mercury(II) ion by making use of gold nanorods (AuNRs) which are found to aggregate after addition of 6-mercaptopurine (6-MP) by forming a covalent Au-S bond. Aggregation is accompanied by a color change to blue. However, the 6-MP induced aggregation is inhibited in the presence of Hg(II) results because of the formation of a more stable Hg-S bond. The different degrees of aggregation of the AuNRs is indicated by variations in the absorption spectra and accompanied by a color change from blue to brown. Under the optimal conditions, the ratio of absorbances at 780 and 665 nm varies in the 1–100 nM Hg(II) concentration range. The effect can also be detected with bare eyes. The limit of detection is 0.48 nM. The method is rapid, sensitive, and does not require sophisticated instrumentation. It was successfully applied to the determination of Hg(II) in spiked water samples.

✉ Ning Bi
bining@hpu.edu.cn

✉ Meihua Hu
humh@hpu.edu.cn

1   College of Chemistry and Chemical Engineering, Henan Polytechnic University, Jiaozuo 454000, People's Republic of China

2   School of Materials Science and Engineering, Henan Polytechnic University, Jiaozuo 454000, People's Republic of China

Introduction

The contamination by heavy metals has aroused extensive public concern since the exposure of the Minamata event in the 1950s. Mercury ion (Hg^{2+}), the most stable inorganic form of mercury, is a hazardous environmental contaminant due to its accumulative and high toxic properties [1]. The maximum allowable level of Hg^{2+} defined by United States Environmental Protection Agency (EPA) is 10 nM in drinking water [2]. The methods for determination of Hg^{2+} include high performance liquid chromatography (HPLC) [3], inductively coupled plasma mass spectrometry (ICPMS) [4], and atomic absorption spectrometry (AAS) [5]. Although these methods provide adequate qualitative and quantitative determination of Hg^{2+}, the sample preparation is complication and the cost of the equipment is high. An inexpensive, sensitive and rapid analytical method is required and many rapid detection methods for determination of Hg^{2+} have been reported. These include fluorescent detection methods [6, 7] colorimetric methods [8], electrochemical sensing methods [9, 10] and surface-enhanced Raman spectroscopy methods [11, 12]. The fluorescence quencher [13, 14], oligonucleotide [15], DNA enzyme [16], and colorimetric probe [17–19] are used as the probe to determination of Hg^{2+}. Among these probes, the colorimetric probe is paid more attention due to Hg^{2+} can be determined based on a color change without using special equipment.

Colorimetric sensors of gold nanoparticles (AuNPs) attracted a great deal of interest for their optical properties [20]. Such as large absorption coefficients, and that characters are depended on the size, shape, and local environment of the nanoparticles [21, 22]. When the distance between AuNPs is shorter than the average diameter of the nanoparticles, the color of the AuNPs is changed, which will cause the change of the absorption spectrum of the AuNPs [23]. Recently, several AuNPs based colorimetric probes have been designed for

determination of Hg^{2+} by modifying nanoparticle surfaces with aptamers [24], peptides [25], proteins [26], fluorophores [27], and others [28, 29]. The preparation of these ligands is easy and inexpensive; the use of commercially available ligands is more desirable for production of cost effective and practical colorimetric assays by eliminating synthesis steps [30]. For instance Hg^{2+} can specifically bind to two thymine bases (T) and mediated the formation of stable DNA duplexes through $T–Hg^{2+}–T$ coordination, various methods have been reported for Hg^{2+} detection based on this recognition system [31, 32]. For gold nanorods (AuNRs),two absorption bands can be observed, one associated with the transverse mode (~520 nm) and the other with the longitudinal mode (usually >600 nm) [33]. The longitudinal plasmon wavelengths are more sensitive to the changes in the dielectric properties of the surroundings and the sensitivity increases with the aspect ratio of the nanorods [34, 35].

In this work, AuNRs were used as colorimetric probe to determination of Hg^{2+} in water. 6-mercaptopurine (6-MP) can be strongly adsorbed on the surface of AuNRs by –SH and induce the aggregation of AuNRs. However, in the presence of Hg^{2+}, 6-MP induced aggregation of AuNRs was inhibited and the aggregation degree is related to the concentration of Hg^{2+}. The separation and concentration of the analyte are not required. Hg^{2+} can be determined with a UV-vis-NIR spectrophotometer and any specialized equipments were not required. This method can be applied to the determination of Hg^{2+} in environmental samples. The experimental results indicated that this method has some benefits, such as sensitivity, simplicity, speediness and stability.

Experimental

Materials

Tetrachloroauric acid ($HAuCl_4·4H_2O$, 99.99%), sodium borohydride ($NaBH_4$, 99%), silver nitrate ($AgNO_3$, 99%), ascorbic acid (AA, 99.7%), cetyltrimethylammonium bromide (CTAB, 99%) and 6-mercaptopurine (6-MP) were purchased from Beijing Ding Guo Biotech. Co. Ltd., China (http://www.bioon.com.cn/show/index.asp?id=123197). The metal salts of analytical reagent grade (>99%) were purchased from Beijing Chemical Reagent Company (Beijing, China, http://www.crc-bj.com/). The stock solution of Hg^{2+} was prepared by dissolving $HgCl_2$ in ultrapure water with several drops of concentrated hydrochloric acid (HCl). The working solution of Hg^{2+} was prepared by diluting the stock solution with ultrapure water. Britton-Robinson (BR) buffer was used to control the acidity of the sample solution. Aqua regia solution was used to clean the glassware. Other chemicals used here were of analytical reagent grade and all the solutions used in this study were prepared with ultrapure water.

Equipments

Absorption spectra were recorded on an Australian GBC Cintra 10e UV-vis-NIR spectrophotometer (http://www.quasi-s.com.sg/) in the wavelength range of 400 to 950 nm. The transmission electron microscope (TEM) image was obtained with a Hitachi H 800 transmission electron microscope (http://www.labbase.net/) operated at an accelerating voltage of 200 kV. The sample was prepared by dropping the analytical solutions on the carbon-coated copper grid and dried at room temperature.

Preparation of AuNRs

AuNRs were synthesized by seed-mediated growth method improved by El-Sayed [36, 37] with slight modification. 5.0 mL of 0.2 M CTAB solution and 5.0 mL of 5×10^{-4} M $HAuCl_4$ solution were mixed in a round bottom flask. Then, 0.6 mL of 0.01 M freshly prepared ice-cold $NaBH_4$ solution was added into the flask. The color of the solution changed from dark yellow to brownish yellow immediately after adding $NaBH_4$, which indicated the formation of gold seeds. The mixed solution was vigorously stirred for 2 min and the flask was placed in a water bath at 25 °C. After 2 h, this seed solution was used for the synthesis of AuNRs. Figure 1a shows the TEM image of gold seeds. The gold seeds were of near monodispersion and homogeneous. The shape of gold seed was spherical and the size of gold seed was between 3 to 5 nm.

3.0 mL of 4 mM $AgNO_3$ solution was added into 50.0 mL of 0.2 M CTAB solution under gentle stirring at 25 °C in a flask. After that, 50.0 mL of 1 mM $HAuCl_4$ solution was added into this solution with gently mixed and the resulted solution was referred as growth solution. Then, 0.7 mL of 0.1 M AA was added into the growth solution under gentle stirring. The color of the growth solution changed from dark yellow to colorless. Finally, 240 μL of the gold seed solution was added into the growth solution at 27–30 °C. The gold seed started growing and as the new atoms join the nanocrystal lattice, they were protected by the surfactant monomers from the solution. Silver ions were adsorbed on the surface of gold nanoparticle in the form of AgBr and restricted the growth on the local surface of the gold nanoparticle. The nanorods were not prepared in the absence of silver ions [37]. Excellent tuning of aspect ratios was achieved by changed the content of $AgNO_3$ in the growth solution [38]. The color of the solution gradually changed within 10–20 min. The resulting solution was kept at 27–30 °C for 24 h to ensure the AuNRs reached full growth. The solution was then centrifuged at 14000 rpm for 20 min twice to remove the excess surfactant CTAB. The resulting deposition containing the rods was redisposed in ultrapure water via the ultrasound and AuNRs solution was obtained.

Fig. 1 TEM images of gold seeds (**a**), AuNRs (**b**), 6-MP-AuNRs (**c**) and 6-MP-AuNRs-Hg^{2+} (**d**) system. Concentration of Hg^{2+}, 100 nM; Concentration of 6-MP, 1.5 μM; pH, 5.0
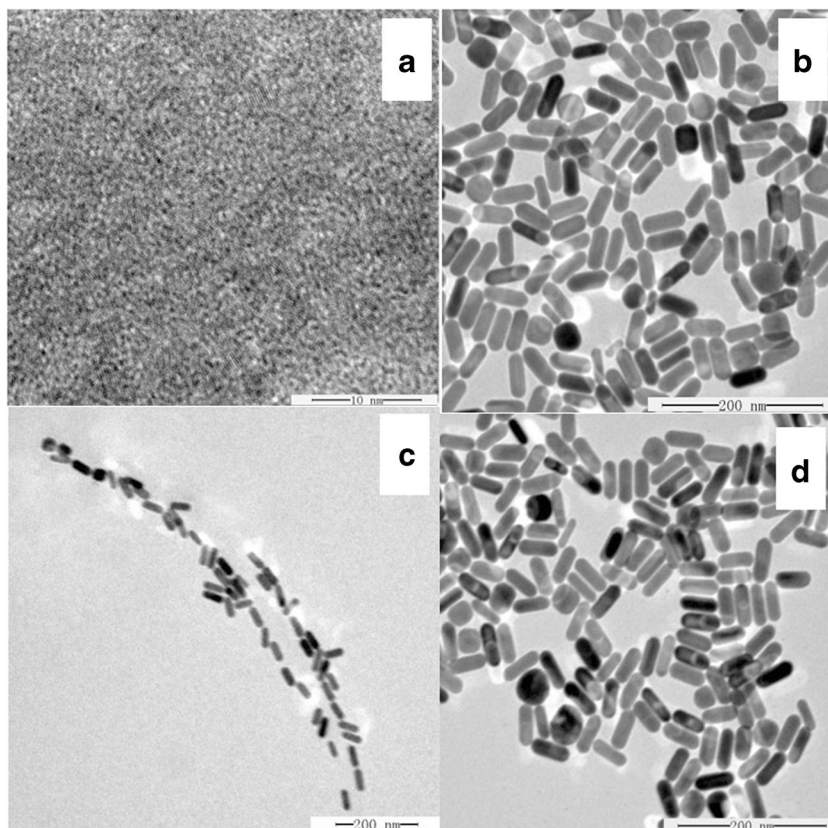
Preparation of water samples

The tap and lake water were collected from the laboratory and Xinyue Lake (Jiaozuo, China), respectively. All the samples collected were spiked with a suitable amount of standard solution of Hg^{2+}. These samples were filtered through a 0.22 μm membrane to remove the suspended particles.

Determination of Hg^{2+}

AuNRs solution was mixed with BR buffer in 5 mL colorimetric tube. 6-MP and the sample solution were added into the colorimetric tube. The obtained solution was diluted to 2.0 mL with ultrapure water and mixed thoroughly with gentle shaken. The resulted solution was incubated for appropriate time at room temperature and the absorption spectrum of the solution was recorded with 1 cm path-length cell.

Results and discussion

Sensing mechanism

Figure 2 show the sensing mechanism of this method. The AuNRs were of monodispersion and the color of the AuNRs appears brownish. After addition of 6-MP into the AuNRs solution in the absence of Hg^{2+}, 6-MP was adsorbed on the surface of AuNRs by the strong covalent interaction between Au and –SH, which destroyed the bilayer structure of AuNRs and caused the aggregation of AuNRs in the solution. The color of the AuNRs solution changed from brownish to blue which can be observed with bare eye. However, in the presence of Hg^{2+}, the color of AuNRs solution changed back to brownish gradually. The absorption spectra of 6-MP-AuNRs remain almost unchanged in the presence of high concentration of Hg^{2+}. The changes in the solution color and UV–vis spectra, induced by the competitive interactions of 6-MP with AuNRs and Hg^{2+}, allowed the colorimetric determination of Hg^{2+} in aqueous solution by bare eyes or UV–vis–NIR spectroscopy.

In this system, 6-MP and Hg^{2+} played the role of aggregation reagent and anti-aggregation reagent, respectively. The aggregation of AuNRs was reversible after adding the 6-MP followed by Hg^{2+}. That is because the covalent bond formed between Hg and sulfur is stronger than that between Au and sulfur. In the presence of Hg^{2+}, 6-MP firstly preferred binding to Hg^{2+} through Hg–S bond and lost the ability to induce the aggregation of AuNRs. The formation of covalent bond of Au-S and Hg-S can be further confirmed by UV-vis spectra (Fig. 3). As shown in Figs. 3 and 6-MP had two absorption bands located at 227 nm and 323 nm, respectively. After addition of 6-MP into the AuNRs solution, the absorbance at
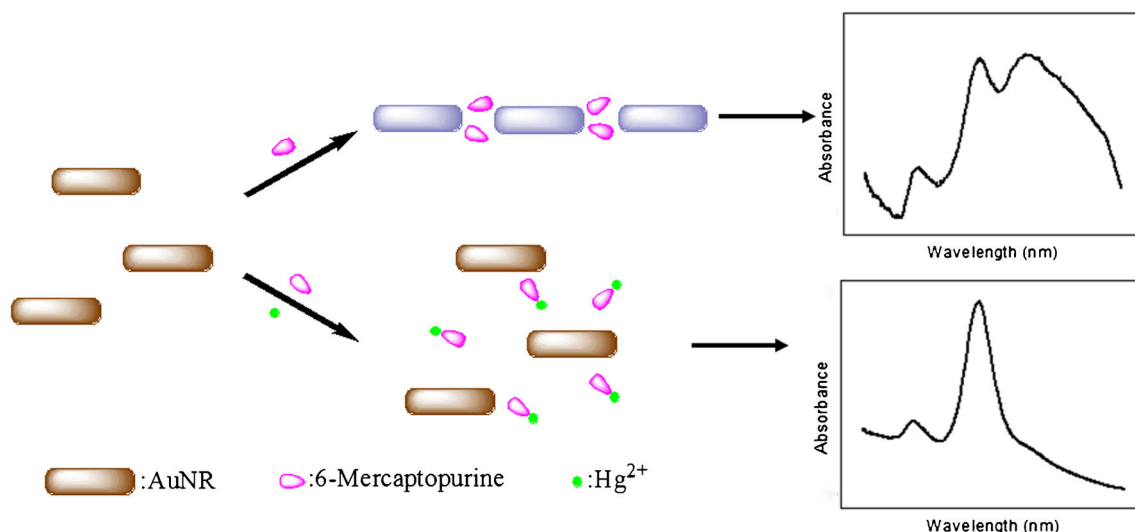
Fig. 2 The schematic mechanism of colorimetric determination of Hg^{2+} based on the inhibition of the aggregation of AuNRs coated with 6-MP

323 nm was increased and the absorption bands located at 227 nm was disappeared, which indicated the formation of covalent bond of Au-S. After addition of 6-MP into the AuNRs solution in the presence of Hg^{2+}, the absorbance at 323 nm decreased with a blue shift to 297 nm and the absorption bands located at 227 nm was disappeared. The UV-vis spectrum indicated the formation of covalent bond of Hg-S and when in the presence of Hg^{2+}, 6-MP firstly preferred binding to Hg^{2+}.

The TEM images (Fig. 1) of AuNRs provides direct evidence of the sensing mechanism. The AuNRs were synthesized by the seed-mediated growth method. CTAB molecule formed bilayer structure on the surface of the AuNRs. In the bilayer structure, two inner and outer layers of surfactants were present. Presumably the inner layer was bound to the gold surface via the headgroups and connected to the outer layer through hydrophobic interactions, while the headgroups of the outer layer were in the aqueous medium [37]. The prepared AuNRs were of near

monodispersion and homogeneous (Fig. 1b). After addition of 6-MP, 6-MP caused the aggregation of AuNRs in the solution and the aggregation had two modes: end-to-end and side-to-side. CTAB molecules had different adsorption ability to different part of the AuNRs. Because CTAB bound to the side was more strongly than to the end of AuNRs, the end of AuNRs had less protection, 6-MP molecules can be easily bound to the ends of AuNRs. After addition of 6-MP, the AuNRs were preferentially assembled in an end-to-end mode to form linear and branched chains (Fig. 1c). However, AuNRs were of near monodispersion in the presence of 6-MP and Hg^{2+} (Fig. 1d), which supported Hg^{2+} inhibit the 6-MP induced aggregation of AuNRs.

Figure 4 shows the absorption spectra of this system. As shown in Fig. 4, the absorption spectra of the prepared AuNRs exhibit two well defined absorption bands: the transverse plasmon band located at 514 nm and the longitudinal plasmon band located at 665 nm. After the addition
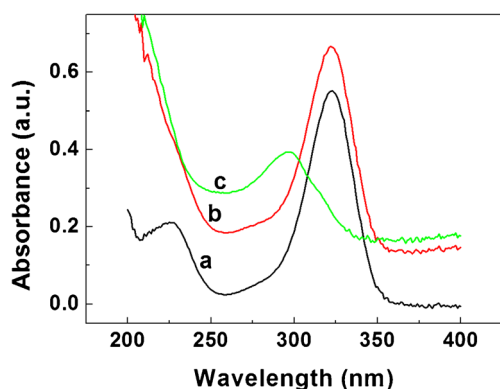

Fig. 3 The absorption spectra of 6-MP (*a*), 6-MP-AuNRs (*b*) and 6-MP-AuNRs-Hg^{2+} (*c*) system. Concentration of 6-MP, 2 μM; Concentration of Hg^{2+}, 100 nM; pH, 5.0
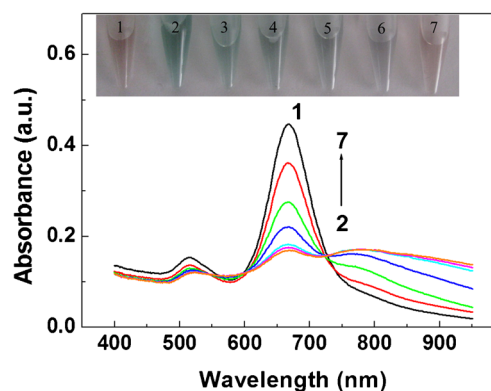

Fig. 4 The absorption spectra and the corresponding photographs of AuNRs (*1*), 6-MP-AuNRs (*2*) and 6-MP-AuNRs-Hg^{2+} (*3–7*) system. Concentrations of Hg^{2+}: (*1*) 0.0, (*2*) 0.0, (*3*) 1.0, (*4*) 5.0, (*5*) 10.0, (*6*) 50.0 and (*7*) 100.0 nM; Concentration of 6-MP, 1.5 μM; pH, 5.0

of 6-MP, a new peak located at 780 nm was observed in the absorption spectra which indicated the aggregation of AuNRs. The absorbance at 780 and 665 nm are related to the amounts of aggregated and dispersed AuNRs, respectively. So, the ratio of the absorbance at 780 nm to that at 665 nm (A_{780}/A_{665}) was used to express the molar ratio of aggregated to disperse AuNRs. After addition of 6-MP in the presence of Hg^{2+}, the absorbance at 780 nm decreased with a blue shift with the increase of Hg^{2+} concentration. However, the absorbance at 665 nm increased with the increase of Hg^{2+} concentration. The changes between the ratios of absorbances in the absence (($A_{780}/A_{665})_0$) and presence (A_{780}/A_{665}) of Hg^{2+} ($\Delta A_{780}/A_{665} = (A_{780}/A_{665})_0 - A_{780}/A_{665}$) was referred to analytical signal. The real photographs of 6-MP-AuNRs-Hg^{2+} system were shown in the inset of Fig. 4. The color change of 6-MP-AuNRs induced by 1.0 nM Hg^{2+} can be viewed with bare eye and the color of AuNRs solution changed back to brownish gradually with the increase of Hg^{2+} concentration.

Optimization of method

The following parameters were optimized: (a) Sample pH value; (b) 6-MP concentration and (c) incubation time. Respective data and Figures are given in the Electronic Supporting Material. We found the following experimental conditions to give best results: (a) sample pH value of 5.0 (Fig. S1, ESM); (b) 6-MP concentration of 1.5 μM (Fig. S2, ESM) and (c) incubation time of 10 min (Fig. S3, ESM).

The selectivity of the method

To evaluate the selectivity of this method, the change of the absorption ratio in the presence of Al^{3+}, Ba^{2+}, Ca^{2+}, Ce^{2+}, Co^{2+}, Cr^{3+}, Fe^{3+}, Fe^{2+}, Mg^{2+}, Mn^{2+}, and Ni^{2+} (all at such as 6 μM), Ag^+, Cd^{2+}, Cu^{2+}, and Pb^{2+} (all at such as 3 μM), was tested under the same experimental conditions when Hg^{2+} concentration was 0.03 μM. The inset of Fig. 5 shows the photographic images of 6-MP-AuNRs solution in the presence of various metal ions and Hg^{2+}. The 6-MP-AuNRs solution remained aggregated with a blue color except for Hg^{2+}. The color of the 6-MP-AuNRs kept brownish after addition of Hg^{2+} due to Hg^{2+} inhibited the aggregation of 6-MP-AuNRs. Figure 5 shows the A_{780}/A_{665} value of 6-MP-AuNRs system in the absence and presence of various metal ions. As shown in Fig. 5, the A_{780}/A_{665} values were similar to that of the blank in the presence of other metal ions, an obvious decrease of A_{780}/A_{665} value only found in the presence of Hg^{2+} relative to that of the blank, which indicating this method had good selectivity for Hg^{2+} detection. Hg^{2+} exhibits much stronger thiophilic tendency than other metal ions. Though the concentration of Hg^{2+} in real water samples was lower or nearly equal to the
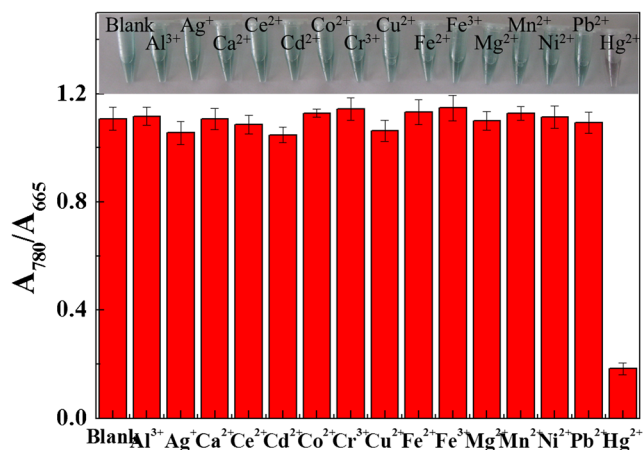

Fig. 5 Photographs (**a**) and A_{780}/A_{665} (**b**) of 6-MP-AuNRs systems in the absence (*blank*) and presence of various metal ions. Concentration of Al^{3+}, Ba^{2+}, Ca^{2+}, Ce^{2+}, Co^{2+}, Cr^{3+}, Fe^{3+}, Fe^{2+}, Mg^{2+}, Mn^{2+}, and Ni^{2+}, 6 μM; Concentration of Ag^+, Cd^{2+}, Cu^{2+}, and Pb^{2+}, 3 μM; Concentration of Hg^{2+}, 0.03 μM. The colors of all systems except for that in the presence of Hg^{2+} are *blue*, the color of the system in the presence of Hg^{2+} is *brownish*

concentration of other metal ions, Hg^{2+} can be determined by this method.

The sensitivity of the method

The capability of this method for quantitatively detecting Hg^{2+} was evaluated by the obvious changes in color and absorption spectrum of 6-MP-AuNRs towards Hg^{2+}. Under the optimum conditions, the calibration curve for determination of Hg^{2+} was constructed. It can be seen from Fig. 6 that the $\Delta A_{780}/A_{665}$ increases linearly with the increase of Hg^{2+} concentration and there is a direct correlation between $\Delta A_{780}/A_{665}$ and the concentration of Hg^{2+} ranging from 1.0 to 100.0 nM. The regression equation is $\Delta A_{780}/A_{665} = 0.04298 + 0.0099 \times 10^9 C$. The corresponding correlation coefficient is 0.997, which indicates that there is good linear relationship between the $\Delta A_{780}/A_{665}$ and Hg^{2+} concentration. The limit of
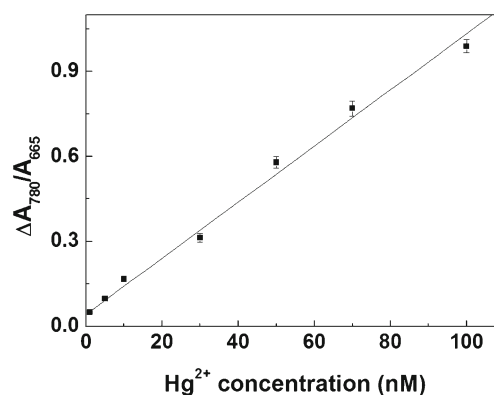

Fig. 6 Relationship between the $\Delta A_{780}/A_{665}$ and Hg^{2+} concentration. Concentration of 6-MP, 1.5 μM; pH, 5.0

Table 1 An overview on recently reported nanomaterial-based methods for determination of Hg^{2+}

Materials	Method	LOD	Linear range	References
Chitosan-functionalized AuNPs	Colorimetric	1.35 μM	9–50 μM	[39]
Gold nanoparticles	Colorimetric	8.4 pM	0.002–0.1 nM	[8]
AuNPs@S-C-dots	Colorimetric	47 nM	50–1000 nM	[40]
Cysteamine modified AuNPs	Colorimetric	30 nM	0.05–3.0 μM	[41]
CA-CdTe QDs/AuNPs/NaCl/aptamer	Fluorescence	0.025 nM	0.05–1.0 nM	[42]
Cysteamine-capped CdTe QDs	Fluorescence	4 nM	6–450 nM	[43]
DNA-AuNCs	Fluorescence	0.083 μM	0.1–100 μM	[44]
AuNRs coated with 6-mercaptopurine	Colorimetric	0.48 nM	1–100 nM	This work

detection (LOD), which corresponds to signal-to-noise ratio 3, is 0.48 nM. The sensitivity and linear range of other methods for determination of Hg^{2+} are listed in Table 1 for comparison. It can be seen that our colorimetric Hg^{2+} sensor showed a superior sensitivity and broader linear range. Compared to AuNPs, the sensitivity of AuNRs was higher.

Analysis of samples

In order to examine the applicability and accuracy of the method, two water samples were collected and analyzed. The water samples were spiked with Hg^{2+} at two concentration levels and the experimental results are listed in Table 2. The recovery values were satisfied (96.7–102.4%) and the RSDs are lower than 3.6%. The results agreed reasonably well with those obtained by ICP-MS (Agilent 7500) measurements, which demonstrates that the method is suitable for Hg^{2+} detection in environmental samples.

Conclusions

In summary, a simple system for colorimetric determination of Hg^{2+} at room temperature based on the inhibition of the aggregation of AuNRs caused by 6-MP was demonstrated. Hg^{2+} can be detected based on the change of the absorbance ratios. This method had a wide linear range of 1 to 100 nM and with a 0.48 nM detection limit. The applicability of this probe has been successfully proven in real samples with good recovery percentages. This method also shows excellent selectivity and

the experimental procedure is quite simple. The samples can be analyzed without previous separation and concentration. This method can be applied for the determination of Hg^{2+} in environmental samples. This detection scheme can also be used to other ions if respective aptamers are available. Therefore, the method holds a great potential for environmental monitoring various metal ions.

Compliance with ethical standards The author(s) declare that they have no competing interests.

References

1. Stoichev T, Amouroux D, Martin-Doimeadios RCR, Monperrus M, Donard OFX, Tsalev DL (2006) Fluorescence spectroscopy of biological tissues-a review. Appl Spectrosc Rev 41:591–619
2. EPA US (2005) Regulatory impact analysis of the clean air mercury rule: EPA-452/ R-05-003
3. Krishna MVB, Castro J, Brewer TM, Marcus RK (2007) Online mercury speciation through liquid chromatography with particle beam/electron ionization mass spectrometry detection. J Anal At Spectrom 22:283–291
4. Leermakers M, Baeyens W, Quevauviller P, Horvat M (2005) Mercury in environmental samples: speciation, artifacts and validation. TrAC Trend Anal Chem 24:383–393
5. Hsu IH, Hsu TC, Sun YC (2011) Gold-nanoparticle-based graphite furnace atomic absorption spectrometry amplification and magnetic separation method for sensitive detection of mercuric ions. Biosens Bioelectron 26:4605–4609
6. Wang RZ, Zhou DL, Huang H, Zhang M, Feng JJ, Wang AJ (2013) Water-soluble homo-oligonucleotide stabilized fluorescent silver nanoclusters as fluorescent probes for mercury ion. Microchim Acta 180:1287–1293
7. Wang ZX, Guo YX, Ding SN (2015) Fluorometric determination of cadmium(II) and mercury(II). Microchim Acta 182:2223–2231
8. Chen YJ, Yao L, Deng Y, Pan DD, Ogabiela E, Cao JX, Adeloju SB, Chen W (2015) Rapid and ultrasensitive colorimetric detection of mercury (II) by chemically initiated aggregation of gold nanoparticles. Microchim Acta 182:2147–2154

Table 2 Determination of Hg^{2+} in water samples

Samples	Added (nM)	Found (nM)	Recovery (%)	RSD (n = 3, %)
Tap water	10.0	9.92	99.2	3.6
	50.0	48.76	97.5	2.1
Xinyue Lake	10.0	9.67	96.7	2.5
	50.0	51.22	102.4	3.4

9. Wang G, He X, Wang B, Zhang X, Wang L (2012) Electrochemical amplified detection of Hg^{2+} based on the supersandwich DNA structure. Analyst 137:2036–2038

10. Zhu Z, Su Y, Li J, Li D, Zhang J, Song S, Zhao Y, Li G, Fan C (2009) Highly sensitive electrochemical sensor for mercury (II) ions by using a mercury-specific oligonucleotide probe and gold nanoparticle-based amplification. Anal Chem 81:7660–7666

11. Senapati T, Senapati D, Kumar Singh A, Fan Z, Kanchanapally R, Chandra Ray P (2011) Chandra ray, highly selective SERS probe for hg (II) detection using tryptophan-protected popcorn shaped gold nanoparticles. Chem Commun 47:10326–10328

12. Wang GQ, Chen LX (2009) Aptameric SERS sensor for Hg^{2+} analysis using silver nanoparticles. Chin Chem Lett 20:1475–1477

13. Cheng X, Li S, Zhong A, Qin J, Li Z (2011) New fluorescent probes for mercury(II) with simple structure. Sensors Actuators B Chem 157:57–63

14. Wang B, Zhuo S, Chen L, Zhang Y (2014) Fluorescent graphene quantum dot nanoprobes for the sensitive and selective detection of mercury ions. Spectrochim Acta Part A 131:384–387

15. Zuo X, Wu H, Toh J, Li SFY (2010) Mechanism of mercury detection based on interaction of single-strand DNA and hybridized DNA with gold nanoparticles. Talanta 82:1642–1646

16. Li T, Li BL, Wang EK, Dong SJ (2009) G-quadruplex-based DNAzyme for sensitive mercury detection with the naked eye. Chem Commun:3551–3553

17. Zarlaida F, Adlim M (2017) Gold and silver nanoparticles and indicator dyes as active agents. Microchim Acta 184:45–58

18. Li X, Su X, Shi Z, Cheng X, Liu S, Zhao Q (2014) Highly selective and reversible colorimetric detection of mercury ions by a hydrophilic cycloruthenated complex in water. Sensors Actuators B Chem 201:343–350

19. Sun MZ, Wu FY, Wu YM, Liu WM (2008) A ditopic colorimetric sensor for fluoride ion based on thiourea mercury complex. Spectrochim Acta Part A 71:814–817

20. Zarlaida F, Adlim M (2017) Gold and silver nanoparticles and indicator dyes as active agents in colorimetric spot and strip tests for mercury(II) ions: a review. Microchim Acta 184:45–58

21. Sepulveda B, Angelome PC, Lechuga LM, Liz-Marzan LM (2009) LSPR-based nanobiosensors. Nano Today 4:244–251

22. Saha K, Agasti SS, Kim C, Li X, Rotello VM (2012) Gold nanoparticles in chemical and biological sensing. Chem Rev 112:2739–2779

23. Mirkin CA, Letsinger RL, Mucic RC, Storhoff JJ (1996) A DNA-based method for rationally assembling nanoparticles into macroscopic materials. Nature 382:607–609

24. Wang Y, Yang F, Yang X (2010) Colorimetric detection of mercury (II) ion using unmodified silver nanoparticles and mercury-specific oligonucleotides. ACS Appl Mater Interfaces 2:339–342

25. Slocik JM, Zabinski JSJ, Phillips DM, Naik RR (2008) Colorimetric response of peptide-functionalized gold nanoparticles to metal ions. Small 4:548–551

26. Xie J, Zheng Y, Ying JY (2010) Highly selective and ultrasensitive detection of Hg^{2+} based on fluorescence quenching of au nanoclusters by Hg^{2+}–au$^+$ interactions. Chem Commun 961−963

27. Liu D, Wang S, Swierczewska M, Huang X, Bhirde AA, Sun J, Wang Z, Yang M, Jiang X, Chen X (2012) Highly robust, recyclable displacement assay for mercuric ions in aqueous solutions and living cells. ACS Nano 6:10999–11008

28. Liu D, Qu W, Chen W, Zhang W, Wang Z, Jiang X (2010) Colorimetric detection of mercury (II) in aqueous media by

quaternary ammonium group-capped gold nanoparticles at room temperature. Anal Chem 82:9606–9610

29. Huang CC, Yang Z, Lee KH, Chang HT (2007) Synthesis of highly fluorescent gold nanoparticles for sensing mercury (II). Angew Chem Int Ed 46:6824–6828

30. Chen L, Xiu FL, Lu W, Chen L (2013) Sensitive and selective colorimetric sensing of Hg^{2+} based on the morphology transition of silver Nanoprisms. ACS Appl Mater Interfaces 5:284–290

31. Miyake Y, Togashi H, Tashiro M, Yamaguchi H, Oda S, Kudo M, Tanaka Y, Kondo Y, Sawa R, Fujimoto T, Machinami T, Ono A (2006) MercuryII-mediated formation of thymine−HgII−Thymine Base pairs in DNA duplexes. J Am Chem Soc 128:2172–2173

32. Lee JS, Han MS, Mirkin CA (2007) Colorimetric detection of mercuric ion (Hg^{2+}) in aqueous media using DNA-functionalized gold nanoparticles. Angew Chem 119:4171–4174

33. Perez-Juste J, Pastoriza-Santos I, Liz-Marz'an LM, Mulvaney P (2005) Gold nanorods: synthesis, characterization and applications. Coord Chem Rev 249:1870–1901

34. Lee KS, El-Sayed MA (2006) Gold and silver nanoparticles in sensing and imaging: sensitivity of Plasmon response to size, shape, and metal composition. J Phys Chem B 110:19220–19225

35. Link S, El-Sayed MA (2005) Simulation of the optical absorption spectra of gold Nanorods as a function of their aspect ratio and the effect of the medium dielectric constant. J Phys Chem B 109:10531–10532

36. Nikoobakht B, El-Sayed MA (2003) Preparation and growth mechanism of gold nanorods (NRs) using seed-mediated growth method. Chem Mater 15:1957–1962

37. Nikoobakht B, El-Sayed MA (2001) Evidence for bilayer assembly of cationic surfactants on the surface of gold nanorods. Langmuir 17:6368–6374

38. Jana NR, Gearheart L, Murphy CJ (2001) Seed-mediated growth approach for shape-controlled synthesis of spheroidal and rod-like gold nanoparticles using a surfactant template. Adv Mater 13:1389–1393

39. Chen ZB, Zhang CM, Tan Y, Zhou TH, Ma H, Wan CQ, Lin YQ, Li K (2015) Chitosan-functionalized gold nanoparticles for colorimetric detection of mercury ions based on chelation-induced aggregation. Microchim Acta 182:611–616

40. Shamsipur M, Safavi A, Mohammadpour Z, Ahmadi R (2016) Highly selective aggregation assay for visual detection of mercury ion based on competitive binding of sulfur-doped carbon nanodots to gold nanoparticles and mercury ions. Microchim Acta 183:2327–2335

41. Ma Y, Jiang L, Mei Y, Song R, Tian D, Huang H (2013) Colorimetric sensing strategy for mercury(II) and melamine utilizing cysteamine modified gold nanoparticles. Analyst 138:5338–5343

42. Hu T, Yan X, Na W, Su X (2016) Aptamer-based aggregation assay for mercury(II) using gold nanoparticles and fluorescent CdTe quantum dots. Microchim Acta 183:2131–2137

43. Ding XJ, Qu LB, Yang R, Zhou YC, Li JJ (2015) A highly selective and simple fluorescent sensor for mercury (II) ion detection based on cysteamine-capped CdTe quantum dots synthesized by the reflux method. Luminescence 30:465–471

44. Zhu SS, Zhuo Y, Miao H, Zhong D, Yang XM (2015) Detection of mercury(II) by DNA templated gold nanoclusters based on forming thymidine-Hg^{2+}-thymidine duplexes. Luminescence 30:631–636